Establishment of a Finite Element Model and Biomechanical Analysis of Different Fixation Methods for Total Talar Prosthesis Replacement

Qian dong Yang
First Affiliated Hospital of Army Military Medical University Sports Medicine Center
Le Chang
First Affiliated Hospital of Army Military Medical University Sports Medicine Center
Xuting Bian
First Affiliated Hospital of Army Military Medical University Sports Medicine Center
Lin Ma
First Affiliated Hospital of Army Military Medical University Sports Medicine Center
Tao Xu
First Affiliated Hospital of Army Military Medical University Sports Medicine Center
Kanglai Tang (tangkanglai@hotmail.com)
First Affiliated Hospital of Army Military Medical University Sports Medicine Center

Research Article

Keywords: Talus prosthesis, Biomechanics, Finite element analysis

Posted Date: May 17th, 2021

DOI: https://doi.org/10.21203/rs.3.rs-515148/v1

Abstract

Back ground A three-dimensional finite element model of the whole foot with high geometric similarity was established and used to simulate the conditions after whole talar prosthesis implantation with several fixation methods, including Screw fixation of subtalar+talus-navicular joint, fixation with screws at only the subtalar joint, and fixation without screws. The biomechanical characteristics of the talus prosthesis were assessed in different gait phases to guide the selection of surgical methods in clinical practice.

Methods With the three-dimensional CT data of a volunteer's foot, Mimics13.0 and Geomagic10.0 software were used to carry out geometric reconstruction of the ankle-related tissues, and Hypermesh10.0 software was used for grid division and material attribute selection. Finally, the data were imported into Abaqus 6.9, and the simulated screw data were applied to different models. Finite element models with different fixation methods were simulated, and the stresses exerted by the human body in three gait phases (heel-strike, midstance and push-off) were simulated. The pressure changes in the articular surface around the talus or the prosthesis, the micromotion of the talus and the prosthesis and ankle motion were measured.

Results Finite element analysis on the biomechanical mechanism showed that screw fixation of the prosthesis in different gait phases mainly increases the pressure on the tibialis articular surface as well as decreases the pressure on the fused articular surface and joint micromotion, which hinders ankle motion. The indicator values were nearly the same in the models of fixation without screws and the normal state.

Conclusion The 3D finite element model created in this study has been verified to be an accurate and reliable model. The biomechanical mechanism varies by fixation method according to finite element analysis. Fixation of the prosthesis without screws yields values most similar to normal values.

Introduction

The talus is the key bony structure connecting the lower limb and foot. Its anatomical structure is complex, and it is the mechanical point of rotation between the lower limb and foot. Stress is concentrated in this area, and the mechanical properties are particularly important [1–3]. Collapsible talus necrosis severely affects individuals' ability to stand and walk, with a disability rate of 100%. Ankle surgeons worldwide mainly perform total talus removal and partial joint fusion at the expense of talus function. Postoperative complications such as adjacent joint degeneration, joint stiffness, and the loss of foot flexibility often occur, and the long-term efficacy of this method is very poor [4, 5].

Due to advancements in modern 3D printing and prosthesis casting technology [6], whole talar prostheses have been used for clinical treatment [7–10], considerably improving the treatment for talus collapse necrosis worldwide. The casting process and surgical indications for the prosthesis are very similar to those used for the conventional method, but the method of prosthesis fixation is different. In

previous studies by Kadakia et al. [11] and Tracy et al. [12], the peritalar soft tissue was directly removed without fixation of the talar prosthesis with screws. In studies conducted in China, screws have been used to fix only the subtalar joint [13] or both the subtalar joint and the subtalar joint at the same time. However, there are no biomechanical studies on the above fixation methods for total talus prostheses.

With finite element analysis, a model with high geometric and physical similarity can be established, which can effectively reflect regional mechanical characteristics. The greatest advantage of this analysis is that there is no damage to organisms, besides, similar research is difficult to perform with objective human or animal experiments [14, 15]. The mechanics of motion of the ankle across the gait cycle are considered. The landing event is the moment when the heel touches the ground, which is the beginning of the supporting phase. In the stance phase, the stress increases and reaches the maximum of the support. The lift-off phase is the beginning of the swing phase. These three stages represent the support and swing phases of the gait cycle and are the three periods that best reflect normal gait and pathological function. Therefore, these three phases were simulated to measure the stress and micromotion of the joints around the whole talar prosthesis as well as the ankle joint motion [16, 17].

In this study, we intended to use the finite element method to simplify the modeling process and preliminarily explore the biomechanical characteristics of the whole talar prosthesis under different fixation methods to guide the selection of the most appropriate fixation methods in clinical practice.

Materials And Methods

Data Collection

A male volunteer aged 30 years, with a height of 177 cm, a body weight of 75 kg and a foot length of 250 mm, participated in this study. An X-ray examination was performed first, and other diseases, such as foot tumors and deformities, were excluded. A 64-slice spiral CT scan of the right ankle was performed, with a slice thickness of 0.60 mm. The data were output and saved in the DICOM format.This study was approved by the institutional review board

ethics committee of the Southwest Hospital Affiliated with the Army Medical University (No. ECFAH2006051), and written informed consent was obtained from the participants,and all methods were performed in accordance with the relevant guidelines and regulations in the methods section.

Finite Element Model Establishment

The data from the CT scan were imported into the three-dimensional reconstruction software Mimics13.0, and the bone tissue and soft tissue were separated by thresholds to establish a geometric model of the whole foot, which was output as an STL file. Then, this file was imported into the reverse engineering software Geomagic Studio10.0, and the noise was removed and smoothed from the model. According to the geometric shape of each joint surface, the cartilage boundary was divided on each bone surface, the surface was fitted, and the resulting file was output in the LEGS format. Then, it was imported into the

finite element preprocessing software Hyperwork10.0, and cartilage was generated according to the generated cartilage boundaries. Based on the ligament anatomical data, a ligament model was established by connecting the ligament attachment points with the three-dimensional arrangement of fiber bundles, and finally, the solid model was subjected to mesh generation, material attribute selection, and other processing steps (Fig. 1). Finally, ABAQUS6.9 software was used for calculation analysis and postprocessing.

Material Parameters

The bony structures and cartilage were modeled as isotropic linear elastic materials, and the ligaments had a nonlinear single-axis connection unit to simulate its characteristic of tension only without compression. The material properties of the bones, cartilage, titanium alloy and ligaments were determined according to previous studies and are listed in Tables 1 and 2. Finally, the finite element model and nodes were built, and they are shown in Table 3.

Table 1
Properties of the bone and cartilage materials.

Material	Elastic modulus	Poisson's ratio
Bone	7300	0.3
Cartilage	12	0.42
Titanium alloy	110000	0.3

Table 2
Material properties of the ligaments.

Ligament	Modulus of elasticity (MPa)	Poisson's ratio	Sectional area (mm2)
AtiF	260	0.4	18.4
PtiF	260	0.4	18.4
AtaFi	255.5	0.4	12.9
PtaFi	216.5	0.4	21.9
CaTi	512	0.4	9.7
AtiTa	184.5	0.4	13.5
PtiTa	99.5	0.4	22.6
TiCa	512	0.4	9.7
TiNa	320.7	0.4	7.1

Table 3
Units and nodes.

	Units	Nodes
Tibia	37876	61152
Fibula	21658	35019
Talus	30422	49181
Calcaneus	47126	74773
Scaphoid bone	8924	14693
Screw	3027	5802
Forefoot	122899	199351

Finally, the finite element model of a normal human foot was successfully established, and then, the following finite element models were established according to the requirements of the different fixation methods.

Boundary Conditions and Loads

There are many ways to divide a gait cycle, but it is usually divided into three phases, heel-strike phase, midstance phase and push-off phase. The axis of flexion-extension and center of rotation were determined in this study according to the research methods reported by previous scholars; the centers of the arcs of the tibialis and peroneal circumferences of the talus pulley were determined, and they were related to the two centers of the circle, the rotation axis, and the midpoint of the two centers of the circle, the rotation center. In research on stress during gait, the load is approximated to be relatively static. Stress during the gait cycle is simulated by applying loads of different sizes and directions. A contact pair is established between the articular surfaces with a coefficient of friction of 0.01. Table 4 shows the reference data for stress in different phases. The normal group model was validated by using data from previous studies.

Table 4
Finite element analysis parameters.

	Heel-strike phase	Midstance phase	Push-off phase
Fx.BW	67.5	225	360
Fy.BW	562.5	907.5	810
Mz.BW.FL	15.375	0	-112.5
BW = 750N, FL = 250 mm			

Results

Three-dimensional finite element models of talar prosthesis fixation with different methods were constructed and analyzed(The specifically constructed finite element model are shown in Fig. 2.), And the distribution of pressure nephograms for three different time phases of the normal group is presented as an example in Fig. 3,and the results regarding the forces on the joints adjacent to the talus were as follows. 1. For the talus joint, the forces in the three phases were uniform under the normal condition. After the talar prosthesis was implanted, the pressure on the talar joint significantly increased, especially in the push-off phase. The pressures on the lower fixed pitch joint with subtalar fixation and subtalar with talar fixation also significantly increased in the heel-strike and midstance phases. The pressure slightly increased with fixation without screws, but the changes in the heel-strike and midstance phases were not significant. 2. For the subtalar joint, under the normal condition, the pressure gradually increased in the heel-strike, midstance, and push-off phases in sequence. The trend was consistent after talar prosthesis replacement, and the fixation method without screws yielded results similar to those under the normal state. When the subtalar joint was fixed, the pressure on the subtalar joint decreased significantly. Therefore, once the subtalar joint was fixed again, the range of motion of the hindfoot was further limited, and the subtalar joint pressure decreased again. 3. For the talar joint, the pressure values increased across the heel strike, midstance and push-off phases. The trend was consistent after talar prosthesis replacement. When screws were not used to fix the prosthesis, the pressure values in the midstance and push-off phases tended to increase. When the screws were used to fix the subtalar joint, the pressure in the three phases of the talar joint decreased. When the talar joint was fixed again, the pressure value decreased further.(Table 5–7)

Table 5
Tibia–talus joint pressure/unit: MPa

	Heel-strike	Midstance	Push-off
Normal	3.494	4.589	5.064
Screw fixation of subtalar joint	4.531	8.663	14.98
Screw fixation of subtalar + talus-navicular joint	4.199	7.585	13.55
Fixation without screws	3.986	5.583	11.08

Table 6
Subtalar joint pressure/unit: MPa

	Heel-strike	Midstance	Push-off
Normal	0.3759	4.342	9.899
Screw fixation of subtalar joint	0.373	1.817	3.295
Screw fixation of subtalar + talus-navicular joint	0.1923	0.4356	1.932
Fixation without screws	0.4354	4.518	13.47

Table 7
Talus-navicular joint pressure/unit: MPa

	Heel-strike	Midstance	Push-off
Normal	0.6529	2.853	6.218
Screw fixation of subtalar joint	0.6555	1.94	2.952
Screw fixation of subtalar + talus-navicular joint	0.3176	1.410	2.498
Fixation without screws	0.5655	4.652	9.306

Regarding slight movement of talus adjacent joint, when a load was applied to simulate the three phases of the gait cycle, we compared the displacement of the talus relative to the adjacent joints, i.e., the tibia, calcaneus and scaphoid, and the results were as follows. The micromovement between joints was reduced by screw fixation, and the situation was particularly obvious when the talus and subtalar joints were fixed. The displacement of the fixation without screw fixation of the talar prosthesis relative to the tibia reduced, probably because the corresponding ligament-supporting connection was lost, but there was no significant increase in relative motion at either the subtalar joint or the subtalar joint.(Table 8–10)

Table 8
Movement relative to the tibia/unit: mm

	Heel-strike	Midstance	Push-off
Normal	0.3633	1.172	1.886
Screw fixation of subtalar joint	0.0978	0.3018	0.4682
Screw fixation of subtalar + talus-navicular joint	0.03776	0.1234	0.2028
Fixation without screws	0.2644	0.8975	1.460

Table 9
Movement relative to the calcaneus/unit: mm

	Heel-strike	Midstance	Push-off
Normal	0.1496	0.3654	0.6168
Screw fixation of subtalar joint	0.04859	0.1431	0.2368
Screw fixation of subtalar + talus-navicular joint	0.03062	0.06863	0.1355
Fixation without screws	0.1814	0.4676	0.7152

Table 10
Movement relative to the scaphoid/unit: mm

	Heel-strike	Midstance	Push-off
Normal	0.1396	0.4291	0.6642
Screw fixation of subtalar joint	0.08954	0.2679	0.4084
Screw fixation of subtalar + talus-navicular joint	0.02407	0.07970	0.1294
Fixation without screws	0.1851	0.5830	0.9182

For ankle joint range of motion, the pressure change between the peri-articular surfaces of the talus and the micromotion of the talus were measured, with the plane axis extending from the central axis of the second metatarsal bone to the heel and the central axis of the tibia used as a reference; the ankle joint was in the neutral position in the neutral phase, in dorsiflexion during the heel-strike phase, and in plantar flexion during the push-off phase. The ankle joint range of motion in the three phases was measured. The results showed that after total talar prosthesis replacement, the ankle joint range of motion changed. Screw fixation greatly limited the range of motion (in line with the characteristics of fusion surgery). There was also limited range of motion in the model with fixation without screws, but this situation was the closest to the normal situation.(Table 11)

Table 11
Ankle joint range of motion/unit: degrees (°)

	Plantar flexion deg	Dorsiflexion deg
Normal	8.57	13.2
Screw fixation of subtalar joint	7.19	10.79
Screw fixation of subtalar + talus-navicular joint	6.92	10.40
Fixation without screws	7.78	11.89

Discussion

The talus plays an important role in the biomechanics of the ankle. Abnormal anatomical structures have large effects on the function of the foot. The ankle joint bears a heavy load in the human body. Any injury to its anatomical structure will affects its stability. Talus osteochondral injuries are common ankle joint injuries that considerably affect the ankle joint [18].

Ischemic collapse necrosis of the talus is challenging to treat [19, 20]. To address this clinical challenge, there are currently three main therapeutic approaches: 1. core decompression, which can preserve joint motion and effectively relieve pain, but the disadvantage is that it is suitable for only patients with early talus necrosis and is not effective for end-stage necrosis [21]. 2. Ankle joint fusion surgery has been suggested to relieve pain and is suitable for patients in almost all stages of necrosis, but it will greatly limit the range of motion of the ankle and affect the quality of life of patients [22]. After the talus collapses, structural bone grafting is often performed during fusion to prevent the force lines of the lower limbs from being affected. If the blood supply around the talus is damaged extensively, tibialis calcaneal fusion or posterior ankle arthrodesis is needed. However, for cases of severe collapse and necrosis of the talus, fusion surgery is not suitable, and in earlier studies, fusion surgery has been proven to be inferior to ankle prosthesis replacement in terms of mobility, efficacy and prognosis [23]. 3. Regarding ankle joint replacement for collapse necrosis of the talus, the requirement of the residual bone mass of the talus is very high to reduce the probability of revision or refusion.

Whole talar prosthesis implantation was first performed and reported by Haenroongroj and Vanadurongwan [24] in 1997, but there were many postoperative complications due to limitations of the casting method. In recent years, with the development of modern computer processing technology, 3D printing technology has been widely used in the clinical practice of orthopedics and has yielded good curative effects.

3D printed, personalized all-talar prostheses can be used for collapse necrosis of the talus. The talus, the core of ankle-hind foot movement, has seven joint surfaces, so it is the first choice for personalized treatment. However, there is always controversy about whether the whole talar prosthesis should be fixed after implantation. Regardless of whether the subtalar joint or subtalar joint is fused, the degree of flexibility and range of motion of the foot are affected [13]. If we choose not to fix the talar prosthesis [11, 12] and use the bony structure of the talus between the ankle points and the ankle-foot complex to obtain self-stability, damage to the adjacent articular cartilage and complications such as prosthesis dislocation may occur. The clinical efficacy of different fixation methods has also been assessed in many studies. Due to relatively short follow-up times and limited number of cases in this study, more scientific and objective data cannot be provided. Therefore, biomechanical studies are urgently needed to verify the biomechanical differences between several different fixation methods so that operators can select the best surgical method.

Traditional orthopedic biomechanical experiments are mainly based on animal or cadaver models. Although the results of these experiments are more reliable than those of simulations, it is often very

difficult to obtain ideal experimental data without changing the physiological state of the model due to limitations in experimental methods, the need to adhere to ethical standards, and the influence of other factors. In recent years, with the development of medical imaging technology and computer processing technology, finite element analysis, a new biomechanical research method, has been widely used in orthopedic mechanics research. Simulation experiments performed by the finite element method have the advantages of a short experimental time, a low cost, the capability of simulating complex boundary conditions, the ability to provide comprehensive mechanical property testing, and good repeatability [14, 15]. In this study, a finite element model was used to simplify and effectively simulate a normal state and different methods of fixing a talar prosthesis. Previous studies have verified that the finite element model in this study was true and effective [25, 26]. The specific biomechanical results are as follows.

It is traditionally believed that fixation must be performed after the prosthesis is inserted, which is similar to fusion surgery. The subtalar joint [13] needs to be fixed or the scaphoid joint needs to be fixed at the same time to stabilize the prosthesis at the ankle. For the prosthesis-bone interface needing screw fixation, a special coating is often used to achieve the biomechanical effect of bone ingrowth. Professor Tang Kanglai's team conducted a series of studies on this topic and has made clinical progress[27–28]. The operation is similar to fusion surgery. Hindfoot motion is limited to a certain extent, which was shown in the finite element model. When loads in different directions were applied, the range of motion of the talus relative to the screw-fixed joint surface decreased; during a simulated gait cycle, the pressure on the tibialis joint increased, and the pressure on the prosthesis-bone interface decreased. Screw fixation does limit the motion between joints and reduce the pressure between fusion joints; however, the finite element results show that the reduced pressure is completely compensated by the tibialis joint. For the talus joint, there is not only a loss of range of motion and an increase in contact pressure but also an increased probability of osteoarthritis in the talus joint surface and an increased possibility of late prosthesis loosening in the long term. However, the effect on ankle range of motion is similar to that of fusion surgery. Clinical research on total talus replacement with a prosthesis indicates that talar prostheses have a better curative effect in the short term [29]. However, studies on bone ingrowth between the bone and prosthesis interface and long-term clinical follow-up studies are currently underway.

Other scholars have used methods other than screw fixation. The first report of using an unfixed method was published by Assal and Stern [30] in 2004, and good curative effects were achieved within the five-year follow-up period. In the heel-strike phase of the gait cycle, when the ankle is in dorsiflexion, the talus was locked upward in the ankle, and there was a force component exerted vertically downward on the calcaneus, so fixation was not required. In the midstance phase, the upper surface of the talar prosthesis incurred a downward stress from the tibia, which exerted a force against the calcaneus and scaphoid at an angle of 140°. The talus was relatively stable and did not need fixation. During the push-off phase, the ankle began to plantar flex, the hindfoot was locked, and the ankle was in the "unlocked state". The moment arm of the talus against the scaphoid increased, and fixation was not required [31]. The finite element model of this study also confirmed the assumption that talar prosthesis fixation without screws yields stable fixation, with biomechanical and ankle range of motion values closest to normal values, and

to the best of our knowledge, no one has conducted relevant studies on self-stability of the talus in the past.

If screw fixation is used, the probability of prosthesis dislocation is relatively low. For cases without screw fixation, dislocation is possible in the following conditions. When the forefoot is off the ground, the Achilles tendon is pulled upward, the hindfoot is plantar flexed, the talus is unlocked forwards, and the anterior ankle is loose. Then, the talus is displaced to large extent forwards and upwards. Due to the containing effect of the scaphoid (bony structure) and the limiting effect of the tibialis anterior and anterior joint capsules (soft tissue) on the prosthesis, the probability of prolapse is relatively low, and the specific biomechanical mechanism needs to be studied further.

Some shortcomings of this study were unavoidable. First, only the bony structures were simulated, and the soft tissues were simplified, which may affect the accuracy of this model to some extent with respect to real conditions. Second, the model was verified by repeating the experiments in previous studies, which does not yield the strongest form of evidence. Therefore, in the future, we plan to verify the results of this finite element study on clinical and cadaveric models. Finally, the surgical method of total talar prosthesis replacement should be carefully considered because the deep layer and the anterior peroneal ligament or the trigonal ligament cannot be reconstructed separately, thus lead to high requirements for the ankle joint bony structure.

Declarations

Ethics approval and consent to participate

This study was approved by the institutional review board ethics committee of the Southwest Hospital Affiliated with the Army Medical University (No. ECFAH2006051)and written informed consent was obtained from all the participants

Consent for publication

Written informed consent for publication was obtained from all participants.

Availability of data and materials

All data included in this study are available upon request by contact with the corresponding author for reasonable demand.

Competing interests

The authors declare there is no conflicts of interest regarding the publication of this paper.

Funding

This work was supported by the Research Fund for National Key Basic Research Development Plan (973) (Grant 2016YFC1100503Y)

Authors' contributions

As the main writer of this article and collector of clinical data, Yang Qiandong and Chang Le are assisted by the first author. Meanwhile, Ma Lin and Bian Xuting have played a great role in the collection and arrangement of clinical data and the collection of reference articles. Tang kanglai and taoxu as commander in chief of the article

Acknowledgement

Thanks to Professor Tao Xu and Professor Tang Kanglai for their guidance and planning for this article.

References

1. Q. Han, Y. Liu, F. Chang et al., “Measurement of talar morphology in northeast Chinese population based on three-dimensional computed tomography,” *Medicine (Baltimore)*, vol. 98, no. 37, p. e17142, 2019.
2. G. Timothy, *Talus Fracture*, StatPearls Publishing, Treasure Island, FL, 2020.
3. A. Flury, A. F. Viehöfer, A. Hoch et al., “Talar neck angle correlates with tibial torsion-Guidance for 3D and 2D measurements in total ankle replacement,” *Journal of Orthopaedic Research* 2020. Doi: 10.1002/jor.24928.
4. S. G. Parekh and R. J. Kadakia, “Avascular necrosis of the talus,” *The Journal of the American Academy of Orthopaedic Surgeons*, 2020. Doi: 10.5435/jaaos-d-20-00418.
5. X. M. Oliva and A. V. Voegeli, “Aseptic (avascular) bone necrosis in the foot and ankle,” *EFORT Open Reviews*, vol. 5, no. 10, pp. 684–690, 2020.
6. T. H. Jovic, E. J. Combellack, Z. M. Jessop and I. S. Whitaker, “3D Bioprinting and the future of surgery,” *Frontiers in Surgery*, vol. 7, p. 609836, 2020.
7. T. A. West and S. M. Rush, “Total talus replacement: case series and literature review,” *The Journal of Foot and Ankle Surgery*, vol. 60, no. 1, pp. 187–193, 2021.
8. J. Huang, F. Xie, X. Tan et al., “Treatment of osteosarcoma of the talus with a 3D-printed talar prosthesis,” *The Journal of Foot and Ankle Surgery*, vol. 60, no. 1, pp. 194–198, 2021.
9. H. Shnol and G. A. LaPorta, “3D printed total talar replacement: a promising treatment option for advanced arthritis, avascular osteonecrosis, and osteomyelitis of the ankle,” *Clinics in Podiatric Medicine and Surgery*, vol. 35, no. 4, pp. 403–422, 2018.

10. D. J. Scott, J. Steele, A. Fletcher and S. G. Parekh, “Early outcomes of 3D printed total talus arthroplasty,” *Foot & Ankle Specialist*, vol. 13, no. 5, pp. 372–377, 2019.
11. R. J. Kadakia, C. C. Akoh, J. Chen, A. Sharma and S. G. Parekh, “3D printed total talus replacement for avascular necrosis of the talus,” *Foot & Ankle International*, vol. 41, no. 12, pp. 1529–1536, 2020.
12. J. Tracey, D. Arora, C. E. Gross and S. G. Parekh, “Custom 3D-printed total talar prostheses restore normal joint anatomy throughout the hindfoot,” *Foot & Ankle Specialist*, vol. 12, no. 1, pp. 39–48, 2018.
13. X. Fang, H. Liu, Y. Xiong et al., “Total talar replacement with a novel 3D printed modular prosthesis for tumors,” *Therapeutics and Clinical Risk Management*, vol. 14, pp. 1897–1905, 2018.
14. S. Mehta, A. Tyler and M. Hast, “Understanding the basics of computational models in orthopaedics: a nonnumeric review for surgeons,” *The Journal of the American Academy of Orthopaedic Surgeons*, vol. 25, no. 10, pp. 684–692, 2017.
15. P. J. Laz and M. Browne, “A review of probabilistic analysis in orthopaedic biomechanics,” *Proceedings of the Institution of Mechanical Engineers Part H*, vol. 224, no. 8, pp. 927–943, 2010.
16. R. O’Sullivan, A. Marron and K. Brady, “Crouch gait or flexed-knee gait in cerebral palsy: is there a difference? A systematic review,” *Gait & Posture*, vol. 82, pp. 153–160, 2020.
17. B. F, C. L.P, M. V et al., “High intensity interval training combined with L-citrulline supplementation: Effects on physical performance in healthy older adults,” *Experimental Gerontology*, vol. 140, pp. 111036, 2020.
18. D. Georgiannos, I. Bisbinas and A. Badekas, “Osteochondral transplantation of autologous graft for the treatment of osteochondral lesions of talus: 5- to 7-year follow-up,” *Knee Surgery, Sports Traumatology, Arthroscopy*, vol. 24, no. 12, pp. 3722–3729, 2016.
19. F. Horst, B. J. Gilbert and J. A. Nunley, “Avascular necrosis of the talus: current treatment options,” *Foot and Ankle Clinics*, vol. 9, no. 4, pp. 757–773, 2004.
20. J. A. Nunley and K. S. Hamid, “Vascularized pedicle bone-grafting from the cuboid for talar osteonecrosis: results of a novel salvage procedure,” *The Journal of Bone and Joint Surgery*, vol. 99, no. 10, pp. 848–854, 2017.
21. A. A. Sultan and M. A. Mont, “Core decompression and bone grafting for osteonecrosis of the talus: a critical analysis of the current evidence,” *Foot and Ankle Clinics*, vol. 24, no. 1, pp. 107–112, 2019.
22. A. Taniguchi, Y. Takakura, K. Sugimoto et al., “The use of a ceramic talar body prosthesis in patients with aseptic necrosis of the talus,” *The Journal of Bone and Joint Surgery British Volume*, vol. 94, no. 11, pp. 1529–1533, 2012.
23. V. Valderrabano, B. Hintermann, B. M. Nigg, D. Stefanyshyn and P. Stergiou, “Kinematic changes after fusion and total replacement of the ankle: part 3: talar movement,” *Foot & Ankle International*, vol. 24, no. 12, pp. 897–900, 2003.
24. T. Harnroongroj and V. Vanadurongwan, “The talar body prosthesis,” *The Journal of Bone and Joint Surgery American Volume*, vol. 79, no. 9, pp. 1313–1322, 1997.

25. J. Li, Y. Wei and M. Wei, “Finite element analysis of the effect of talar osteochondral defects of different depths on ankle joint stability,” *Medical Science Monitor*, vol. 26, p. e921823, 2020.
26. C. H. Lu, B. Yu, H. Q. Chen and Q. R. Lin, “Establishment of a three-dimensional finite element model and stress analysis of the talus during normal gait,” Nan Fang Yi Ke Da Xue Xue Bao, vol. 30, no. 10, pp. 2273–2276, 2010
27. Mu Mi Duo,Yang Qian Dong,Chen Wan et al. Three dimension printing talar prostheses for total replacement in talar necrosis and collapse.[J].Int Orthop, 2021, undefined: undefined.
28. Yang QD, Mu MD, Tao X, Tang KL. Three-dimensional printed talar prosthesis with biological function for giant cell tumor of the talus: A case report and review of the literature. World J Clin Cases 2021; 9(13): 0–0
29. T. Harnroongroj and T. Harnroongroj, “The talar body prosthesis: results at ten to thirty-six years of follow-up,” The Journal of Bone and Joint Surgery American Volume, vol. 96, no. 14, pp. 1211–1218, 2014.
30. M. Assal and R. Stern, “Total extrusion of the talus. A case report,” *The Journal of Bone and Joint Surgery American Volume*, vol. 86, no. 12, pp. 2726–2731, 2004.
31. V. L. Giddings, G. S. Beaupré, R. T. Whalen and D. R. Carter, “Calcaneal loading during walking and running,” *Medicine and Science in Sports and Exercise*, vol. 32, no. 3, pp. 627–634, 2000.

Figures

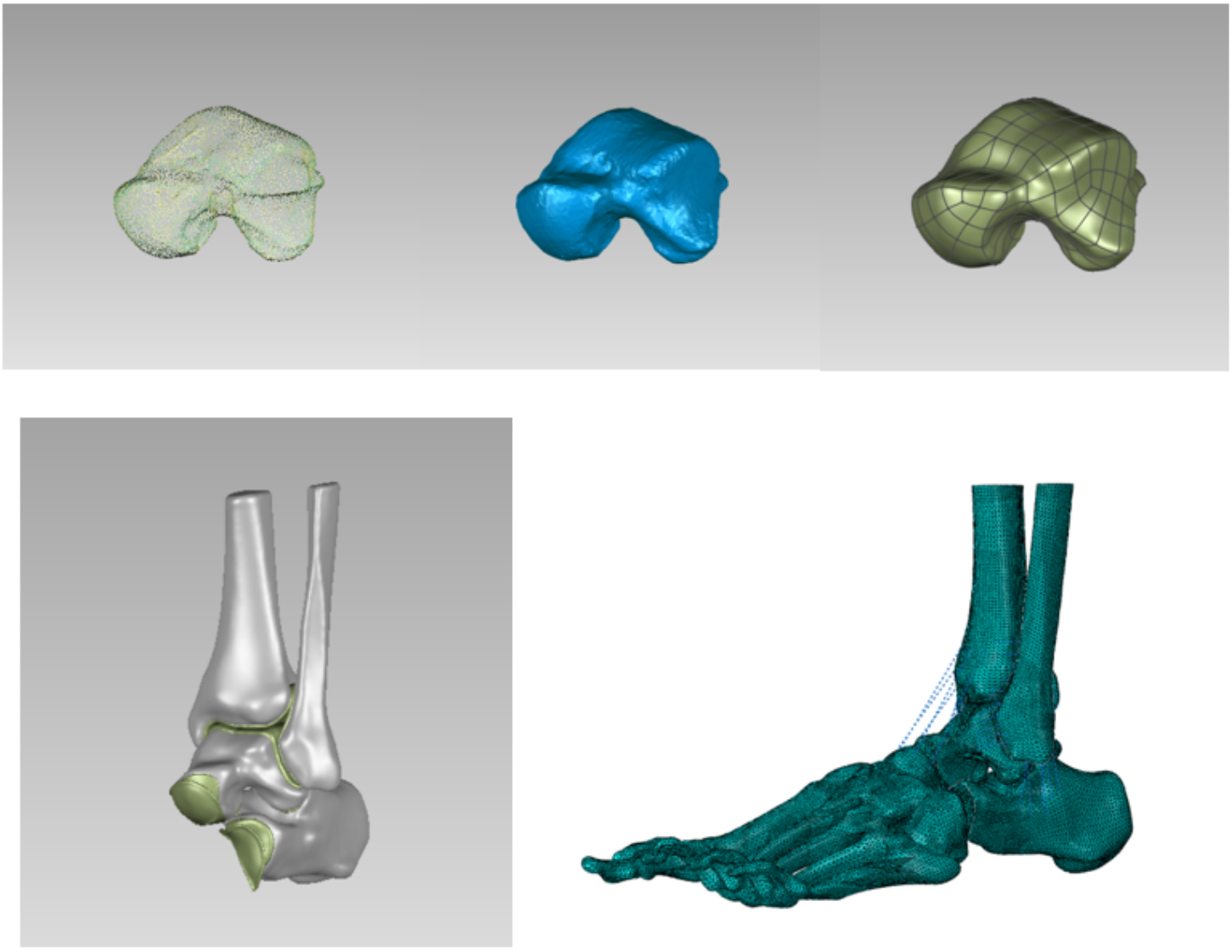

Figure 1

Schematic diagram of the finite element modelling process.

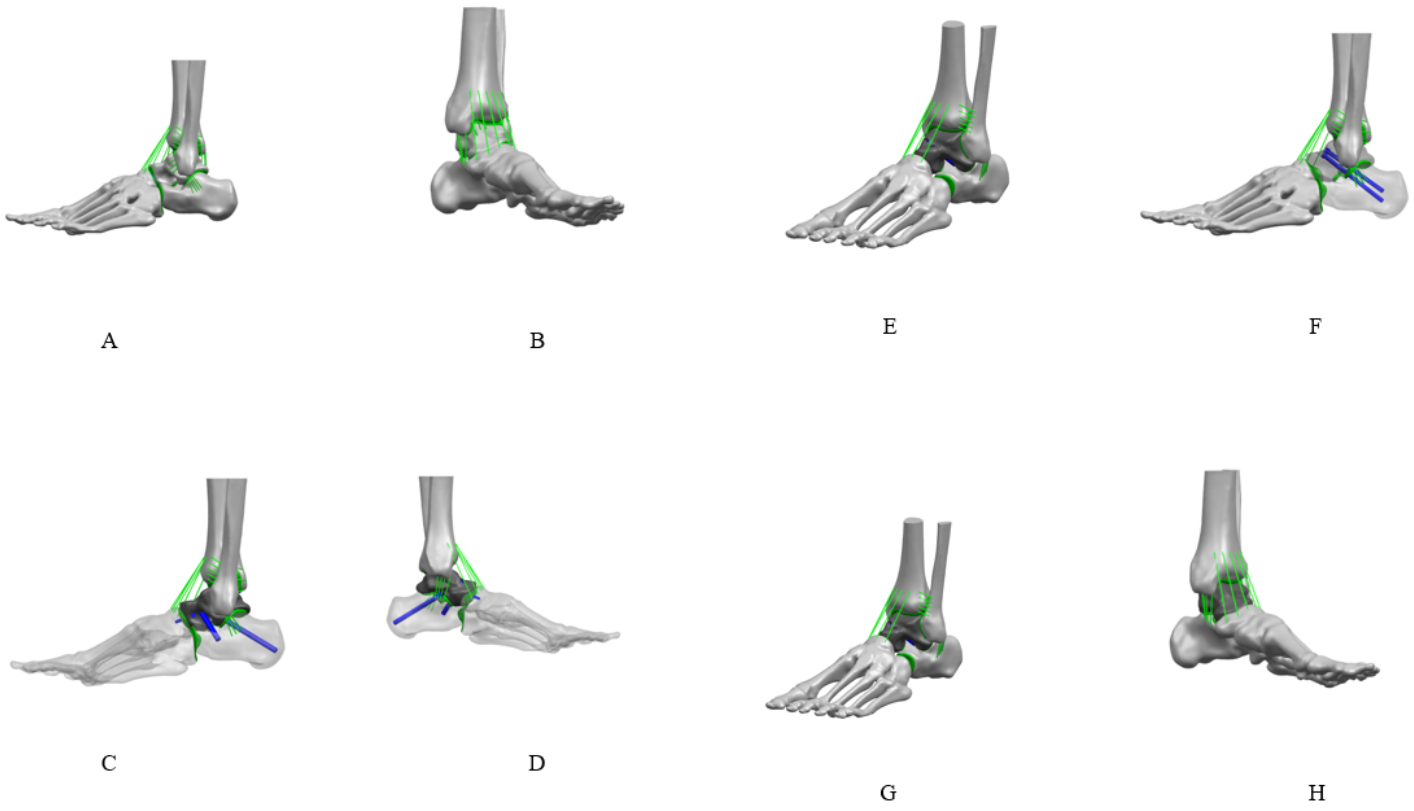

Figure 2

A-B:Normal group,C-D:Fixed talus-navicular joint+subtalar joint group,E-F:Fixed subtalar joint group，G-H， No fixation group.

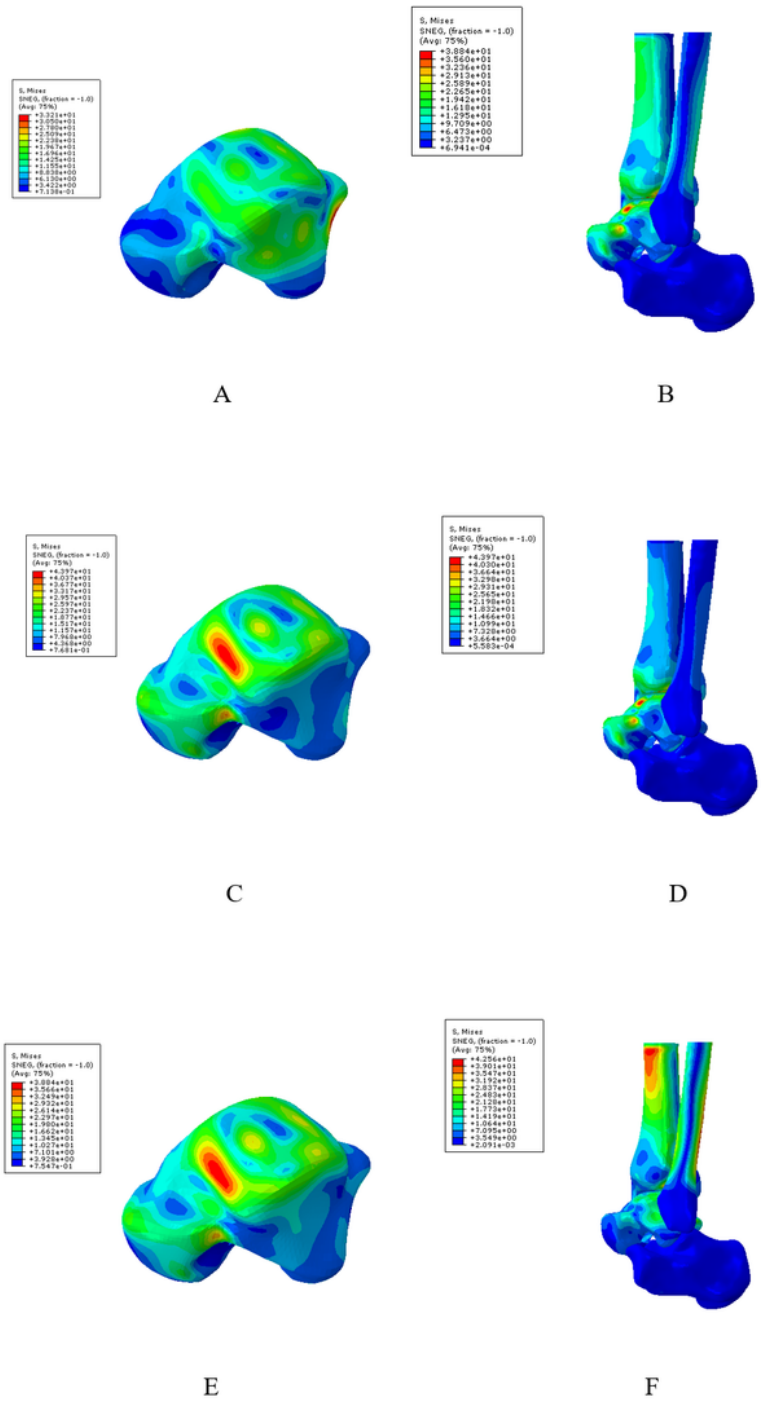

Figure 3

A-B:Mechanical characteristics of normal group at Heel-strike stance;C-D:Mechanical characteristics of normal group at Midstance;E-F：Mechanical characteristics of normal group Push-off stance